Cell Tissue Res (2002) 307:337–345
DOI 10.1007/s00441-001-0503-x

REGULAR ARTICLE

**Jane L. Fisher · Jacqueline F. Schmitt
Monique L. Howard · P. Scott Mackie
Peter F. M.Choong · Gail P. Risbridger**

An in vivo model of prostate carcinoma growth and invasion in bone

Received: 11 September 2001 / Accepted: 20 November 2001 / Published online: 14 February 2002

Abstract Prostatic carcinoma affects 1 in 11 men and targets bone with sclerotic metastases. The study of prostate carcinoma growth in bone has been hampered by the lack of suitable animal models. We have developed an in vivo model of prostate carcinoma growth in bone by inoculating three human prostate carcinoma cell lines (PC-3, DU-145, and LNCaP) into the tibia of congenitally athymic mice. Developing tumors were analyzed by radiographic, histologic, immunohistochemical, and in situ hybridization examination. Seven of the nine PC-3 inoculated mice and all (9/9) of the DU-145 inoculated mice developed tumors in the injected limb. In contrast, inoculation with LNCaP cells failed to produce tumors (0/9). Radiologically, the tumors had a mixed sclerotic/lytic appearance with extracortical extension. All the PC-3 tumors invaded the bone marrow cavity, cortical bone, and surrounding soft tissue. The DU-145 tumors were confined to the bone marrow cavity in 7/9 animals. CK18 and Ki67 localization identified the human tumor cells and their proliferative activity, respectively. The PC-3- and DU-145-induced tibial tumors expressed α(1)I procollagen and osteopontin mRNA, to varying degrees. All the tumors demonstrated an up-regulation of osteoclasts at the bone/tumor interface compared with the control limbs. Thus, this is a reliable and reproducible in vivo model of prostate carcinoma growth in bone enabling the study of the interactions that occur between prostate cancer cells and bone at an important part of the metastatic cascade, namely, growth and invasion at a distant site.

Keywords Animal model · Prostate · Bone · Cancer · Mouse (BALB/c, *nu/nu*)

J. L. Fisher and J. F. Schmitt contributed equally to this work. These studies were partially supported by a Monash University Research Fund Grant in conjunction with Novogen Limited, 140 Wicks Road, North Ryde, Sydney, Australia 2113, Australian Orthopaedic Association Level 2, Culwulla Chambers, 67 Castlereagh St. Sydney, Australia, 2000, and Victorian Orthopaedic trust, c/o Australian College of Surgeons, Spring St, Melbourne, 3000.

J.L. Fisher (✉) · M.L. Howard · P.S. Mackie · P.F. M.Choong
Orthopaedic Department, 3rd Floor Daly Wing,
St. Vincent's Hospital, Fitzroy, 3065, Australia

J.F. Schmitt · G.P. Risbridger
Centre for Urological Research,
Monash Institute of Reproduction and Development,
Clayton, Victoria, 3168, Australia

Present address:
J. Fisher, Orthopaedic Department, St. Vincents Hospital,
41 Victoria Pde, Fitzroy, Victoria, Australia 3068,
e-mail: agjfisher@bigpond.com
Tel.: +61-3-9288 2480, Fax: +61-3-9416 2676

Introduction

Cancer of the prostate is one of the most common male malignancies, affecting approximately 1 in 11 men (Landis et al. 1998; Pisani et al. 1999). Prostate cancer metastases occur in bone in approximately 75% of patients with advanced disease (Coleman 1997). Metastases from prostate cancer are generally sclerotic in nature, although bone resorption also appears to be accelerated in these tumors (Adami 1997). Despite its prevalence, the mechanisms involved in the development of prostate metastases in bone remain incompletely understood (Scher and Chung 1994), thus limiting the treatment of prostate cancer bone metastases to the management of pain, pathologic fracture, and marrow invasion (Mundy 1997).

The process of metastasis involves a complex series of interactions between the host and tumor cells (Aznavoorian et al. 1993). Tumor cells must escape from the primary tumor, degrade the extracellular matrix, and migrate to and arrest at distant sites, where they subsequently invade the surrounding tissue and establish as a secondary tumor. The propensity for prostate carcinoma to colonize bone suggests that the microenvironment in bone promotes the growth of prostate cancer cells at the latter stage of the metastatic cascade.

Little is known about the factors that promote prostate carcinoma colonization and growth in bone, although several hypotheses have been suggested. Paget (1889) has proposed the "seed and soil" mechanism for breast

cancer, which emphasizes the importance of the selective migration of the tumor ("seed") to the secondary site ("soil"; Zetter 1990). Furthermore, it has been suggested that the high incidence of prostate cancer metastases in the lumbar spine may be attributable to preferential retrograde venous flow through the vertebral venous system (Berrettoni and Carter 1986). More recently, it has been proposed that prostate carcinoma acquires osteoblast-like properties in the bone microenvironment, which may enhance the ability of prostate cancer cells to invade and grow in bone (Koeneman et al. 1999). In addition, the presence of osteolytic destruction, particularly in late-stage or aggressive tumors (Coleman 1997), is strong evidence for an osteoclast-mediated resorptive process during prostate cancer growth in bone.

A model of prostate cancer growth in bone is essential for studying the cellular and molecular interactions that underlie the behavior of prostate skeletal metastases. To date, in vivo studies of intraosseous prostate cancer cell growth have been hampered by the lack of suitable animal models. Earlier models lacked the histological features of clinical prostate cancer or produced low rates of metastasis to bone (Shevrin et al. 1989; Thalmann et al. 1994). More recently, researchers have used intrafemoral inoculations of human prostate cancer cells PC-3 and LNCaP cells to examine tumor growth (Soos et al. 1997; Wang and Stearns 1991; Wang et al. 1999).

We have previously established an in vivo model of osteosarcoma by using inoculation of human osteosarcoma cells into the tibiae of nude mice (Fisher et al. 2001). The aims of the current study have been to expand this technique and the work carried out by previous researchers and to develop and characterize a reproducible model of prostate carcinoma growth and invasion in bone. This model allows us to focus on an important step of the metastatic cascade of prostate carcinoma, namely, growth and invasion in bone, and enables us to explore the interactions that occur between the tumor cells and the osteoblasts and osteoclasts. Using this model, we have compared the growth and invasive capabilities of the human prostate carcinoma cell lines, PC-3, DU-145, and LNCaP in bone by means of histologic and immunological techniques. Additionally, we have examined the pattern of expression of bone-related genes, α1 (type I) procollagen (COL) and osteopontin (OPN), to assess the possible role of these matrix proteins in tumor establishment and growth in bone.

Materials and methods

Animals and animal maintenance

Congenitally athymic male nude mice (BALB/c, *nu/nu*, Animal Resource Centre, Perth, WA) were purchased germ-free at 2–3 weeks of age and housed in the Orthopaedic Department Sterile Facility. Animals were kept for at least 1 week in the facility before experimental manipulation. They were kept in a sterile environment in cages with beds of sterilized soft wood granulate and were fed irradiated rat chow ad libitum with autoclaved and acidified (pH 2.5) tap water. An artificial cycle of 12 h light/12 h dark was maintained in the room where the animals were kept. A maximum of five mice were kept in each box, and all manipulations were performed with sterile techniques in a laminar-flow hood in the animal facility. Experiments were performed with animals at 4 weeks of age.

Before tumor inoculation, radiographic examination, and sacrifice, mice were anesthetized with an intraperitoneal mixture of ketamine (50 mg/kg), xylazine (5 mg/kg), and acepromazine (0.75 mg/kg). The St. Vincent's Hospital Animal Ethics Committee approved all experimental procedures, and animal care was in accordance with NHMRC animal ethics guidelines.

Cell culture

The human prostate cancer cell lines, PC-3, DU-145, and LNCaP were obtained from the American Tissue Culture Collection (Rockville, Md.). The cells were cultured in DMEM supplemented with 10% heat inactivated fetal calf serum (all from Gibco), harvested by trypsinization (0.25% trypsin, 0.02% EDTA) and washed three times by centrifugation in serum-free α-DMEM. Cell concentration and viability were determined in 0.2% trypan blue solution by using a hemocytometer.

Based on their different rates of growth, final cell concentrations of 4.7×10^6 cells/ml for the PC-3 cell line, 7.7×10^6 cells/ml for the DU-145 cell line, and 5.6×10^6 cells/ml for the LNCaP cell line were used. Cells were kept at 4°C until being used for mouse inoculation (0–2 h).

Intratibial implantation of prostate cancer cell suspensions

Nine animals in each group were anesthetized, and the left leg was cleaned with 70% ethanol. The prostate cancer cells were aspirated into a 25-µl syringe fitted with a 25-gauge needle. The needle was inserted through the cortex of the anterior tuberosity of the tibia, 3 – 5 mm down the diaphysis of the tibia, and 10 µl of cell suspension was injected. The right leg, which served as a control, was inoculated with media alone in an identical manner.

Radiographic examination

Mice were anesthetized, and radiograms were taken by means of a mammography unit (Picker, LoRad) with Fuji computer radiography cassettes and printed to hard copy films. Radiograms were taken at the time of sacrifice.

Tissue processing

Mice were killed by an anesthetic overdose at 4 weeks post-inoculation, and the left and right legs were dissected. The limbs were immediately fixed in 4% paraformaldehyde in phosphate-buffered saline (PBS) at 4°C for 24 h and then transferred into a sterile decalcification solution (15% EDTA/0.5% paraformaldehyde in PBS, pH 8.0) for 3 weeks. Following fixation, the tissues were paraffin-embedded for histologic examination, immunohistochemistry, and in situ hybridization studies. All specimens were handled under sterile conditions to avoid degradation of RNA in the sample. Hematoxylin and eosin (H/E) staining assessed tumor development in these limbs.

Antibodies and immunohistochemistry

Immunohistochemistry was performed on representative tibial tumors (five tumors per cell line). Serial antibodies were used to identify the human prostate cancer cells in mouse tissues. These included the human epithelial cell marker anti-cytokeratin (CK) 18 (NovoCastra Laboratories Ltd, Newcastle upon Tyne, UK) and the proliferation marker anti-Ki67 (DAKO, Carpiteria, Calif.). Immunohistochemistry involved the indirect avidin-biotin-enhanced horseradish-peroxidase method. Antigen retrieval was performed

after dewaxing and dehydration of the tissue sections (5 µm) by autoclaving them for 1 min at 121°C in Target Retrieval Solution (DAKO). Sections were cooled to room temperature, treated with 6% hydrogen peroxide in methanol for 30 min, and blocked with Superblock (DAKO) for 1 h at room temperature. Sections were then incubated with the primary antibody to CK18 (diluted 1:20) at 4°C overnight or the antibody to Ki-67 (diluted 1:50, DAKO) at room temperature for 2 h. Sections were washed in PBS and incubated with biotinylated horse antimouse IgG1 (CK18, Zymed Laboratories, San Francisco, Calif.) or biotinylated goat antirabbit IgG (Ki-67, Zymed Laboratories) for 1 h. After further washes, the antibodies were detected with the Vectastain Elite ABC kit (Vector Laboratories, Burlingame, Calif.) and color-developed with 3,3'-diaminobenzidine tetrahydrochloride (Liquid substrate kit, Zymed Laboratories).

Synthesis of riboprobes

Probes were labeled with digoxigenin (DIG) by using an RNA labeling kit (Boehringer Mannheim, Mannheim, Germany) according to the manufacturer's instructions. The COL RNA riboprobe was obtained by subcloning a 1.6-kb *Pst*I fragment of rat COL cDNA (from Dr. J. Bateman, Royal Children's Hospital, Melbourne, Australia) into pSPT 18 or pSPT 19 plasmids. These plasmid vectors were linearized by using *Eco*RI or *Hin*dIII for pSPT 19 and pSPT 18, respectively. They were transcribed with T7 RNA polymerase to generate 1.6-kb antisense and sense strands, respectively. A 1.6-kb *Xba*I–*Xho*I insert of human OPN cDNA (from Dr. L. Fisher, National Institute of Dental Research, USA) was linearized with *Xba*I or *Xho*I and transcribed with T7 or T3 RNA polymerase to generate antisense and sense riboprobes, respectively.

RNA preparation and Northern analysis

Sub-confluent cultures of human PC-3, DU-145, and LNCaP prostate cancer cells and rodent UMR 106–01 osteoblast like cells were washed twice with PBS and harvested with TRIzol (2 ml per 10-cm^2 plate). Total RNA was prepared according to the manufacturer's instructions (Gibco BRL); 20 µg RNA was electrophoresed on a 1.5% agarose-formaldehyde gel and then transferred to a GeneScreen membrane. The filters were hybridized overnight with the DIG-labeled riboprobes in 50% formamide, 5×SSC (1×SSC = 150 mM sodium chloride and 15 mM sodium citrate, pH 7.0), 2% block reagent (Boehringer), 0.02% SDS, and 0.1% N-laurosarcosine at 65°C. The filters were washed to a stringency of 0.1×SSC at 65°C and exposed to Kodak XAR-5 X-ray film (Eastman Kodak, Rochester, N.Y.) with an intensifying screen. The RNA gel loading was standardized by 18S.

In situ hybridization

In situ hybridization was performed on tibiae (left and right) from five mice inoculated with PC-3 cells and five mice inoculated with the DU-145 cells, as previously described (Fisher et al. 2000). Briefly, 5-µm-thick paraffin sections were mounted on slides, dewaxed with xylene, and rehydrated in ethanol before being rinsed in water. The sections were deproteinized with 0.2 M HCl, digested with 2 µg/ml proteinase K, and fixed in 4% paraformaldehyde in PBS. Prehybridization was performed at 65°C for 1 h in hybridization buffer. The digoxigenin-labeled probe was then applied to each section, and the slides were incubated for 16–18 h at 65°C in a humidified chamber. Excess probe was removed by incubation with 25 µg/ml RNase A, and the slides were washed in decreasing concentrations of SSC at 37°C. Detection of the hybridized probe was with the alkaline-phosphatase-coupled antidigoxigenin antibody according to the manufacturer's instructions. Negative control slides were pretreated with 150 µg/ml RNase A prior to hybridization or hybridized with sense digoxyigenin-labeled riboprobes and then treated as described above. Where possible, sections from PC-3-induced tumors, DU-145-induced tumors, and control limbs were hybridized on the same slide and in the same experiment. All solutions were pre-treated with pyrocarbonic acid diethyl ester. Following in situ hybridization, tissue sections were counter-stained with Nuclear Fast Red.

Tartrate-resistant acid phosphatase staining

An acid phosphatase leukocyte kit (Sigma Diagnostics, St. Louis, USA) was used to detect the tartrate-resistant acid phosphatase (TRAP) in osteoclasts, in accordance with manufacturer's instructions.

Fig. 1 Radiographs of tibiae of athymic nude mice following intratibial inoculation of human prostate cancer cells. Representative radiographs of the right (control, *C*) and left (test, *T*) legs of mice inoculated with PC-3, DU-145 and LNCaP cells, respectively, 4 weeks post-inoculation. The tibial tumors of mice inoculated with the PC-3 and DU-145 cell lines have a mixed sclerotic/lytic appearance (*arrow*) with extracortical extension

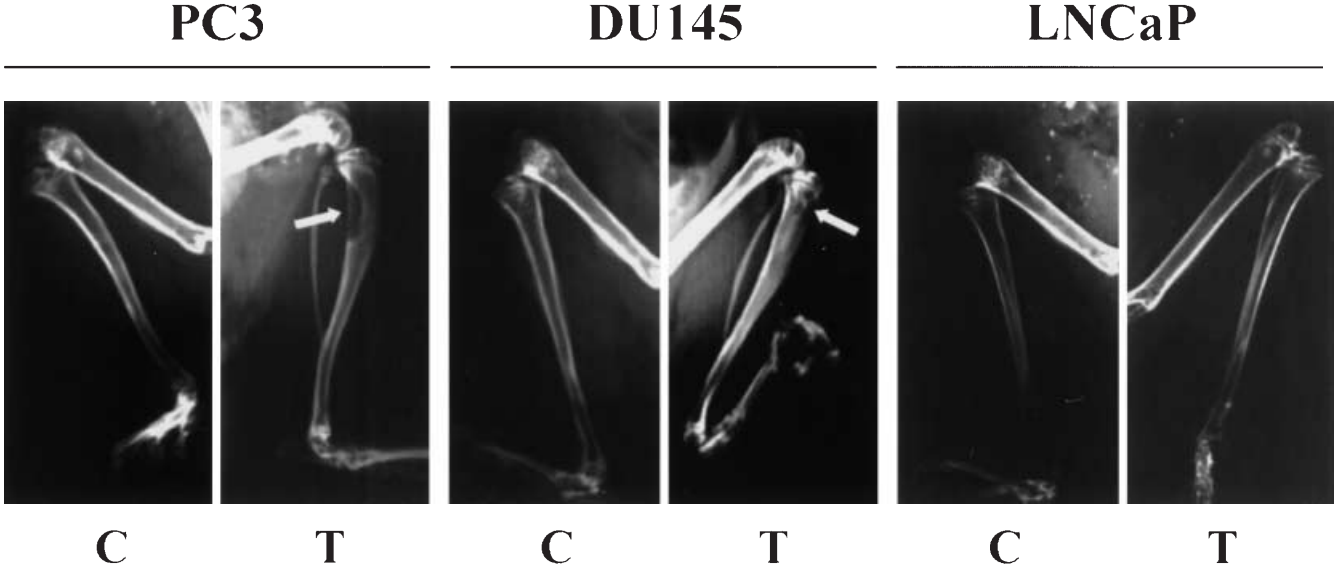

Results

Radiology

Tumor growth in the tibiae of the nude mice was assessed radiologically and histologically 4 weeks post-inoculation. Seven of the nine mice inoculated with PC-3 human prostate cells and all of the nine mice inoculated with the DU-145 human prostate cancer cells developed radiologically detectable tibial tumors, at 4 weeks post-inoculation (Fig. 1). Radiologic features characteristic of human prostate carcinoma, including mixed sclerotic and lytic lesions, were evident in the metaphysis of the inoculated tibiae. In contrast, there were no obvious radiologic changes observed in the tibiae of mice (*n*=9) inoculated with the LNCaP prostate cancer cells (Fig. 1).

Histology

Histologic examination of these tissues revealed intramedullary growth of the tumor within the metaphysis in seven of the nine mice inoculated with the PC-3 cell line and in all of the nine mice inoculated with the DU-145 prostate cancer cell line, as observed radiologically. Specifically, inoculation with the PC-3 prostate cancer cells resulted in tibial tumors that had expanded within the medulla and had entirely displaced the normal hematopoietic cells. These tumors consisted of PC-3 prostate cancer cells and fibroblast-like cells, heterogeneously distributed throughout the tumor mass. The tumors were also associated with areas of trabecular bone destruction and cortical breach, with tumor invasion into the surrounding soft tissue (Fig. 2A). There were also areas of new bone formation toward the periphery of the tumors.

The DU-145 cells produced tumors that were largely confined within the bone marrow cavity. In each tumor, nests of tumor cells were observed within the surround-

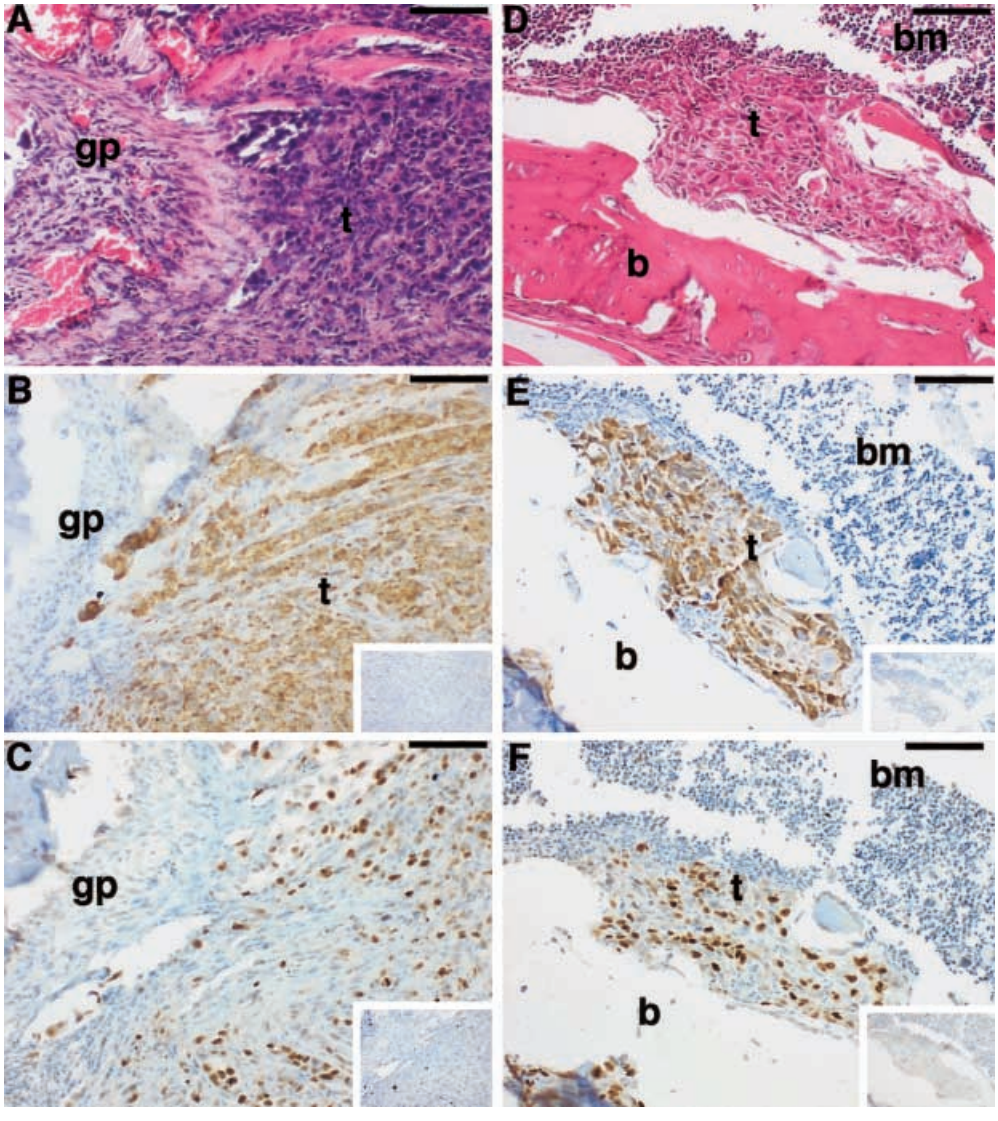

Fig. 2 Specific identification of proliferating human prostate cancer cells PC-3 (**A–C**) and DU-145 (**D–F**) growing in mouse tibiae, 4 weeks post-inoculation (*b* bone, *bm* bone marrow, *gp* area adjacent to the remaining growth plate, *t* tumor mass). H/E-stained longitudinal tibial cross sections showing a tumor mass of PC-3 cells (**A**) and DU-145 cells (**D**) growing within the bone marrow cavity. The human origin of the cells was confirmed by immunohistochemistry for human cytokeratin 18 (**B, E**) and the proliferative nature of the tumor mass was demonstrated by the presence of immunoreactive Ki-67 (**C, F**). The controls for each were negative (*insets*). *Bar* 100 µm

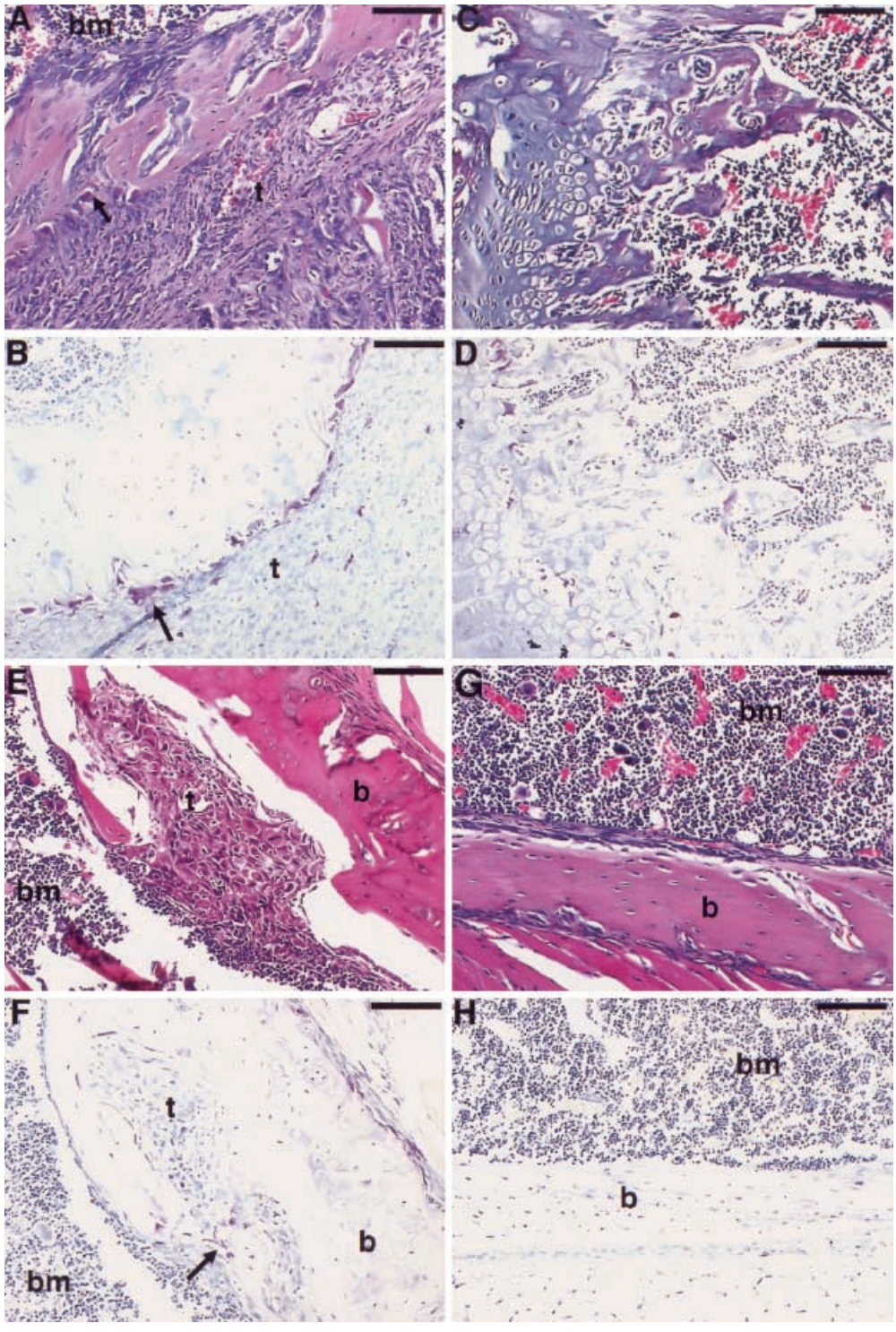

Fig. 3A–H Micrographs of PC-3 and DU-145 cells in the tibiae of athymic nude mice, 4 weeks post-inoculation (*b* bone, *bm* bone marrow, *t* tumor mass). **A–D** Mice inoculated with PC-3 cell line. **A** H/E-stained section of tumor cells within the metaphysis of the injected limb, with osteoclasts (*arrow*) at the bone/tumor interface. **B** TRAP staining of tumor cells, identifying the osteoclasts (*arrow*) at the tumor/bone interface. **C, D** H/E staining and TRAP staining, respectively, of the right (control) leg from the same mouse. **E–H** Mice inoculated with DU-145 cell line. **E** H/E stained section of tumor cells within the tibiae. **F** TRAP stain of tumor cells, identifying the osteoclasts (*arrow*) on the tumor/bone interface. **G, H** H/E staining and TRAP staining, respectively, of the right (control) leg from the same mouse. *Bar* 100 µm

ing trabecular bone (Fig. 2D), which was otherwise intact. Isolated tumor nests consisted entirely of DU-145 prostate cancer cells and were surrounded by spindle-shaped cells. Only three of the nine mice inoculated with DU-145 cells had tumors that had breached the cortical bone and invaded the surrounding soft tissue. In contrast, no tibial tumors were observed in the mice (n=9) inoculated with the LNCaP human prostate cancer cell line, 4 weeks post-inoculation (results not shown), as observed by radiologic analysis.

Although inoculation of two of the nine mice with the PC-3 prostate cancer cells failed to produce tibial tumors, the characteristics of PC-3-induced tumors, such as cortical bone destruction and invasion into the surrounding tissue, were typical of more aggressive tumors. These results highlighted a difference in the invasive ca-

pabilities and growth characteristics of the PC-3, DU-145, and LNCaP cell lines.

Immunohistochemistry

Immunostaining of the tumor masses for the human-specific epithelial cell marker CK18 confirmed the presence of PC-3 cells (Fig. 2B) and DU-145 cells (Fig. 2E) in the inoculated tibiae. The tumors consisted of heterogeneous cell populations of human and mouse cells, as the immunostaining was not uniform throughout the tumor masses. The specificity of the human CK18 antibody was confirmed by the failure to detect CK18 in mouse keratinocytes (data not shown). Proliferation of the human tumor cells could be demonstrated by the presence of immunoreactive Ki-67 in the nuclei of the PC-3 cells (Fig. 2C) and DU-145 cells (Fig. 2F).

Localization of osteoclasts

We examined whether there was an increase in osteoclast recruitment in these tibial tumors compared with the control limbs. Tibiae inoculated with the PC-3 prostate cancer cells demonstrated a relative increase in the number of osteoclasts, as indicated by large multinucleated TRAP-positive cells in lacunae, on the bone surface adjacent to the tumor cells (Fig. 3A, B) compared with the control tibiae (Fig. 3C, D). Similarly, there was an increase in the number of osteoclasts present at the bone/tumor interface in tibiae inoculated with the DU-145 prostate cancer cells (Fig. 3E, F) compared with the control tibiae (Fig. 3G, H).

Expression of osteoblast-related proteins in vitro

To determine the expression of COL and OPN mRNA in the prostate cancer cell lines prior to intratibial inoculation, we performed RNA analysis in vitro. There was no COL or OPN RNA detected in the PC-3, DU-145, or LNCaP cell lines (results not shown). In comparison, the UMR106–01 cell line expressed RNA for both COL and OPN.

Expression of osteoblast-related proteins in situ

We examined COL and OPN gene expression in the tibial tumors compared with the control limbs. Localization of the expression of COL and OPN mRNA in the prostate tumor masses in bone was achieved by in situ hybridization by using DIG-labeled riboprobes.

In the PC-3-induced tumors, high levels of signal for COL mRNA were localized to the tumor cells and the osteoblasts at the bone/tumor interface (Fig. 4A). In comparison, there was only a low level of expression of COL mRNA in the lining osteoblasts in the corresponding control limbs (Fig. 4B). Moderate signals for COL mRNA were also evident, heterogeneously distributed throughout the tumor mass in all of the tibiae inoculated with PC-3 cells. The corresponding COL mRNA RNase control was negative.

Moderate signals for OPN mRNA were uniformly expressed throughout the tumor mass (Fig. 4C) in all of the PC-3-induced tibial tumors examined. There was no difference in the levels of OPN mRNA at the bone/tumor interface compared with normal bone in the control tibiae (results not shown).

The tumors formed by inoculation with the DU-145 cells expressed low to moderate levels of COL mRNA, which was particularly prominent in cells at the bone/tumor interface (Fig. 4D). This expression was greater than that observed in normal bone in the control limbs (Fig. 4E). OPN mRNA was also expressed at low levels in the tumor masses of mice inoculated with DU-145 cells (Fig. 4F). Overall, the expression of COL and OPN mRNA was lower than that observed in the PC-3 tumors. Similar OPN expression was observed in normal bone in the control limb (results not shown).

Discussion

We have established a reliable and reproducible model of prostate cancer growth and invasion in bone by using intratibial inoculation with the human prostate cancer cell lines PC-3 and DU-145 into nude mice. Previous models including tail-vein, intra-cardiac, or orthotopic injection result in a low incidence of osseous metastasis formation, are complex, or do not adequately reflect the human disease (Shevrin et al. 1989; Thalmann et al. 1994; Wu et al. 1998). In contrast, intratibial inoculation results in a high incidence of tumor establishment in bone, is easy to perform, and results in tumors that are radiologically and histologically similar to those encountered clinically.

This model represents an important step of the metastatic cascade, namely, the establishment and growth of tumor cells at a distant site (bone). It also allows us to explore, in vivo, the interactions that occur between prostate cancer cells, osteoblasts, and osteoclasts.

The PC-3 cells formed heterogeneous tumors that replaced the bone marrow and that resulted in the destruction of the cortical bone and invasion into the surrounding soft tissue, whereas the DU-145-induced tumors were largely confined within the bone marrow cavity. In contrast, the LNCaP cells failed to produce tibial tumors, suggesting a greater biological aggressiveness of the former two cell lines. Certainly, differences in the tumorigenicity and metastatic potential of these prostate cancer cell lines have previously been reported following orthotopic inoculation (Rembrink et al. 1997; Stephenson et al. 1992). Furthermore, Soos and co-workers (1997), using intrafemoral inoculation, reported that, after an initial increase, the LNCaP cells regressed and were eventually replaced by the host bone marrow.

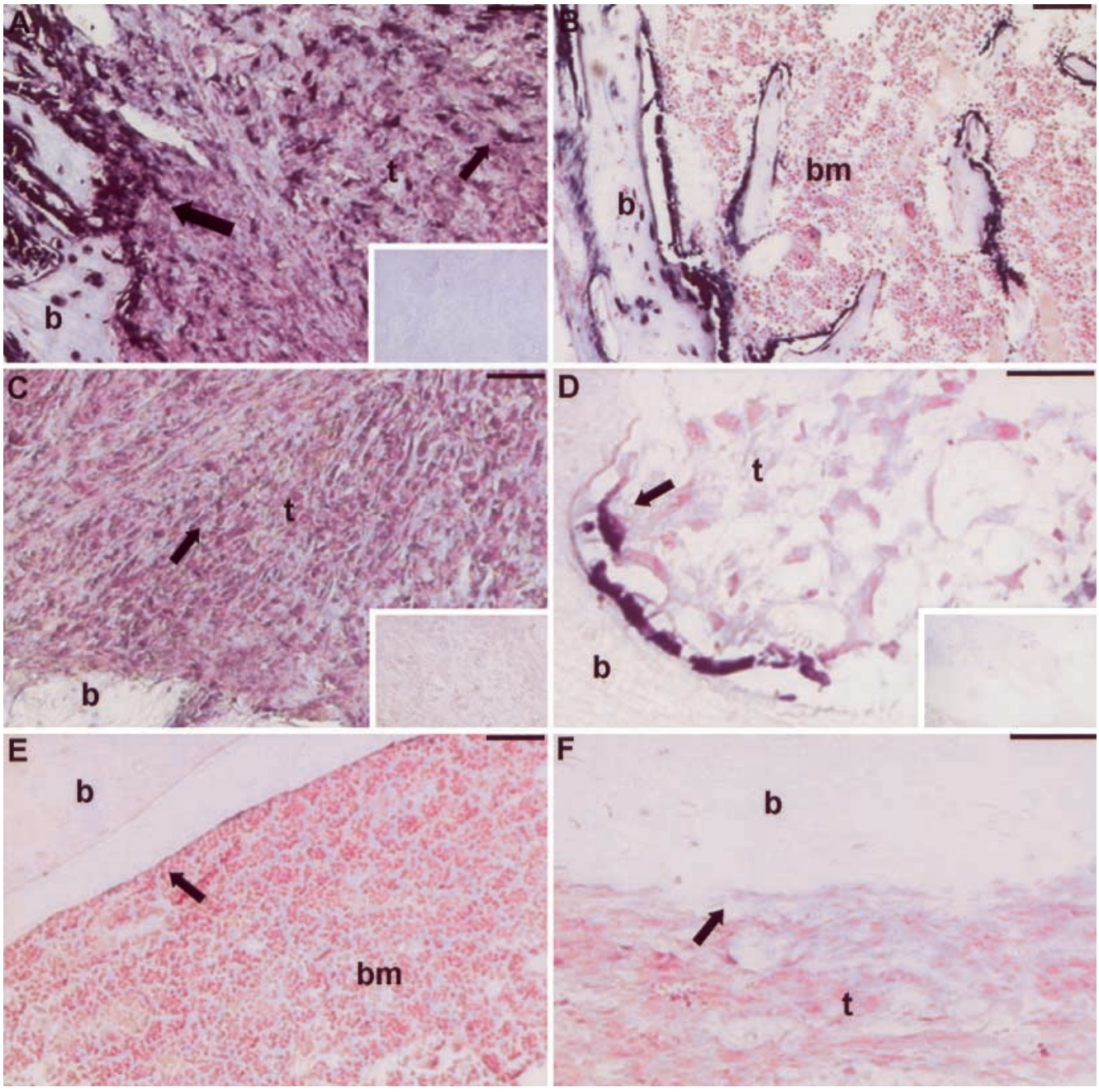

Fig. 4A–F Localization of expression of bone related factors in PC-3 and DU-145 cells growing in the tibiae of athymic nude mice at 4 weeks post inoculation (*b* bone, *bm* bone marrow, *t* tumor mass). **A–C** PC-3 cell line. **A** COL mRNA expression was localized to the tumor mass (*small arrow*) and was particularly prominent at the bone/tumor cell interface (*large arrow*). **B** COL mRNA on right (control) tibia. **C** OPN mRNA expression (*arrow*) localized to the PC-3 human prostate tumor cell line growing within the metaphysis. **D–F** DU-145 cell line growing in bone. **D** Expression of COL mRNA was localized to the bone/tumor interface within the bone marrow cavity of mice inoculated with DU-145 tumor cells. **E** COL mRNA (*arrow*) expression at the same area in the right (control) tibia. **F** Low levels of OPN mRNA expression (*arrow*) in the DU-145 cells growing in the mice tibiae. *Bar* 100 μm

There is a notable increase in the population of osteoclasts around the advancing tumor front in both the PC-3- and DU-145-induced tumors. This may be a remodeling response to bone destruction. Nonetheless, this recruitment may be important since recent work suggests that osteoclast-mediated osteolysis is a necessary antecedent step in the development of osteoblastic metastases (Adami 1997). In this regard, Yoneda et al. (2000) have demonstrated an inhibition of the development of osteoblastic metastases from mammary carcinoma when osteoclastic lysis is inhibited by bisphosphonate treatment. This inhibition has not been demonstrated in prostate carcinoma, and studies are currently underway in our laboratory to assess this interaction in our model. It

is important to resolve the role of osteoclast osteolysis in the growth of prostate carcinoma in bone because effective methods for osteoclast inhibition, such as bisphosphonates, are available.

The capacity of prostate carcinoma to adhere to the extracellular bone matrix is highly dependent on the cell-cell and cell-matrix interactions that occur at the secondary site (Tan et al. 1999; Wilson et al. 1999). OPN is an extracellular protein that is found in high levels in normal bone, amongst other tissues (Denhardt and Guo 1993). It plays an important role in cellular attachment, via the GRGDS sequence that is recognized by several integrins, particularly the $\alpha_v\beta_3$ integrin (Varner and Cheresh 1996). Previous studies have demonstrated increased OPN expression in a number of transformed cell lines (Chambers et al. 1992; Senger et al. 1989), and OPN mRNA has been localized to macrophages in a number of human tumors, including prostate carcinoma, in which approximately 50% of tumors are positive for OPN (Tozawa et al. 1999).

OPN is expressed in PC-3, and to a lesser extent, DU-145 tumor masses in our model. In contrast, no OPN mRNA has been detected in either the PC-3 or the DU-145 cell line by Northern analysis, suggesting a possible up-regulation of OPN mRNA in the tibial tumors. OPN may play a role in the adhesive interactions that occur at the bone/tumor interface during the initial establishment and subsequent growth of the tumor. It is tempting to speculate whether tumor cells express OPN themselves or whether they are modulating the expression of OPN in adjacent bone and stromal cells to increase cell adhesion and hence motility and invasion.

We have also examined the expression of COL mRNA in prostate cancer cells growing in bone. Type I collagen is the major component of the mineralized matrix of bone, although it is also present in many connective tissues. The release of procollagen peptides into the circulation has been shown to correlate with the development of bone metastases in a number of human cancers, including prostate cancer (Kylmala et al. 1993), and we have previously shown the over-expression of type I collagen in invasive breast carcinomas (Fisher et al. 2000).

In this study, we have localized COL mRNA expression to the tumor mass in the PC-3-induced and, to a lesser extent, DU-145-induced tumors. The expression is relatively uniform throughout the tumors, although COL mRNA expression tends to be greater at the bone/tumor interface in the PC-3-induced tumors. It is unclear whether the tumor cells themselves are producing COL mRNA or whether they are acting indirectly to increase COL expression in the adjacent osteoblasts and bone stromal cells.

Simpson et al. (1985) have demonstrated that conditioned media from PC-3 cell lines stimulate mitogenesis in a phenotypically osteoblastic osteosarcoma cell line and increase collagen synthesis in fetal rat calvaria in vitro. Similarly, Koutsilieris et al. (1994) have reported that the co-incubation of PC-3 cells with MG-63 osteoblast-like cells results in an increased density of Type 1 collagen around MG-63 cells adjacent to PC-3 cells. In this regard, the increased expression of COL mRNA that we have observed at the PC-3 bone/tumor interface suggests that there may be an up-regulation of osteoblast proliferation, possibly by a tumor-induced paracrine or other mechanism. Alternatively, increased COL expression may simply reflect tumor cell origin or degradation of the extracellular matrix.

The increased expression of COL mRNA may also reflect an affinity of the tumor cells for bone. Hullinger et al. (1998) have demonstrated that prostate tumor cells directly adhere to the surrounding trabecular bone, and the over-expression of Type I collagen and OPN that we have observed may be, in part, responsible for this. In this regard, the effect of the up-regulation of tumor OPN and COL may be important not only for bone targeting, but also for conferring a survival advantage through enhanced attachment and local migration.

In conclusion, we have developed a reliable and reproducible in vivo model of prostate carcinoma growth and invasion in bone, a model that we have employed to explore the cellular and molecular interactions that occur between prostate cancer cells, osteoblasts, and osteoclasts. The determination of the factors that promote the preferential targeting of bone by prostate carcinoma should facilitate the development and treatment strategies to minimize or inhibit tumor progression in patients who have developed metastases.

References

Adami S (1997) Bisphosphonates in prostate carcinoma. Cancer 80:1674–1679

Aznavoorian S, Murphy AN, Stetler-Stevenson WG, Liotta LA (1993) Molecular aspects of tumor cell invasion and metastasis. Cancer 71:1368–1383

Berrettoni B, Carter J (1986) Mechanisms of cancer metastasis to bone. J Bone Joint Surg Am 68A:308–312

Chambers AF, Behrend EI, Wilson SM, Denhardt DT (1992) Induction of expression of osteopontin (OPN; secreted phosphoprotein) in metastatic, ras-transformed NIH 3T3 cells. Anticancer Res 12:43–47

Coleman RE (1997) Skeletal complications of malignancy. Cancer 80:1588–1594

Denhardt DT, Guo X (1993) Osteopontin: a protein with diverse functions. FASEB J 7:1475–1482

Fisher J, Field C, Zhou H, Harris T, Henderson M, Choong P (2000) Urokinase plasminogen activator system gene expression is increased in human breast carcinoma and its bone metastases – a comparison of normal breast tissue, non-invasive and invasive carcinoma and osseous metastases. Breast Cancer Res Treat 61:1–12

Fisher J, Mackie P, Zhou H, Howard M, Choong P (2001) The expression of the urokinase plasminogen activator system in metastatic osteosarcoma: an in vivo model. Clin Cancer Res 7: 1654–1660

Hullinger T, McCauley L, Dejoode M, Somerman M (1998) Effects of bone proteins on human prostate cancer cell lines in vitro. Prostate 36:14–22

Koeneman K, Yeung F, Chung L (1999) Osteomimietic properties of prostate cancer cells: a hypothesis supporting the predilection of prostate cancer metastasis and growth in the bone environment. Prostate 39:246–261

Koutsilieris M, Sourla A, Pelletier G, Doillon C (1994) Three-dimensional type 1 collagen gel system for the study of osteoblastic metastases produced by metastatic prostate cancer. J Bone Min Res 9:1823–1832

Kylmala T, Tammela T, Risteli L, Risteli J, Elomaa I (1993) Evaluation of the effect of oral clondrate on skeletal metastases with type I collagen metabolites. A controlled trial of the Finnish Prostate Cancer Group. Eur J Cancer 29A:821–825

Landis SH, Murray T, Bolden S, Wingo PA (1998) Cancer statistics, 1998. Cancer J Clin 48:6–29

Mundy GR (1997) Mechanisms of bone metastasis. Cancer 80: 1546–1556

Paget S (1889) The distribution of secondary growths in cancer of the breast. Lancet 1:571–573

Pisani P, Parkin DM, Bray F, Ferlay J (1999) Estimates of the worldwide mortality from 25 cancers in 1990. Int J Cancer 83: 18–29

Rembrink K, Romijn J, Van der Kwast T, Rubben H, Schroder F (1997) Orthotopic implantation of human prostate cancer cell lines: a clinically relevant animal model for metastatic prostate cancer. Prostate 31:168–174

Scher HI, Chung LW (1994) Bone metastases: improving the therapeutic index. Semin Oncol 21:630–656

Senger DR, Perruzzi CA, Papadopoulos A (1989) Elevated expression of secreted phosophoprotein I (osteopontin, 2ar) as a consequence of neoplastic transformation. Anticancer Res 9:1291–1299

Shevrin D, Gorny K, Kukreja S (1989) Patterns of metastasis by the human prostate cancer cell line PC-3 in athymic nude mice. Prostate 15:187–194

Simpson E, Harrod J, Eilon G, Jacobs JW, Mundy GR (1985) Identification of a messenger ribonucleic acid fraction in human prostatic cancer cells coding for a novel osteoblast-stimulating factor. Endocrinology 117:1615–1620

Soos G, Jones RF, Haas GP, Wang CY (1997) Comparative intraosseal growth of human prostate cancer cell lines LNCaP and PC-3 in the nude mouse. Anticancer Res 17:4253–4258

Stephenson RA, Dinney CP, Gohji K, Ordonez NG, Killion JJ, Fidler IJ (1992) Metastatic model for human prostate cancer using orthotopic implantation in nude mice. J Natl Cancer Inst 84:951–957

Tan MI, Strunck E, Scholzen T, Gerdes J, Vollmer G (1999) Extracellular matrix regulates steady-state mRNA levels of the proliferation associated protein Ki-67 in endometrial cancer cells. Cancer Lett 140:145–152

Thalmann GN, Anezinis PE, Chang SM, Zhau HE, Kim EE, Hopwood VL, Pathak S, Eschenbach AC von, Chung LW (1994) Androgen-independent cancer progression and bone metastasis in the LNCaP model of human prostate cancer. Cancer Res 54:2577–2581

Tozawa K, Yamada Y, Kawai N, Okamura T, Ueda K, Kohri K (1999) Osteopontin expression in prostate cancer and benign prostatic hyperplasia. Urol Int 62:155–158

Varner JA, Cheresh DA (1996) Integrins and cancer. Curr Opin Cell Biol 8:724–730

Wang M, Stearns ME (1991) Isolation and characterization of PC-3 human prostatic tumor sublines which preferentially metastasize to select organs in S.C.I.D. mice. Differentiation 48:115–125

Wang X, An Z, Geller J, Hoffman R (1999) High-malignancy orthotopic nude mouse model of human prostate cancer LNCaP. Prostate 15:182–186

Wilson DF, Jiang DJ, Pierce AM, Wiebkin OW (1999) Oral cancer: role of the basement membrane in invasion. Aust Dent J 44:93–97

Wu TT, Sikes RA, Cui Q, Thalmann GN, Kao C, Murphy CF, Yang H, Zhau HE, Balian G, Chung LW (1998) Establishing human prostate cancer cell xenografts in bone: induction of osteoblastic reaction by prostate-specific antigen-producing tumors in athymic and SCID/bg mice using LNCaP and lineage-derived metastatic sublines. Int J Cancer 77:887–894

Yoneda T, Michigami T, Yi B, Williams PJ, Niewolna M, Hiraga T (2000) Actions of bisphosphonate on bone metastasis in animal models of breast carcinoma. Cancer 88:2979–2988

Zetter B (1990) The cellular basis of the site-specific tumor metastasis. N Engl J Med 322:605–612